Report

257430177: Atmospheric Chemistry - Nitrosamine Photolysis

Deliverable D3+D4

Author
René Wugt Larsen,
University of Copenhagen

SINTEF Materials and Chemistry
Process Technology
2011-11-18

SINTEF

SINTEF Materialer og kjemi
SINTEF Materials and Chemistry

Address:
Postboks 4760 Sluppen
NO-7465 Trondheim
NORWAY

Telephone:+47 73593000
Telefax:+47 73597043

info.mk@sintef.no
www.sintef.no/mk
Enterprise /VAT No:
NO 948007029 MVA

Report

257430177: Atmospheric Chemistry - Nitrosamine Photolysis

Deliverable D3+D4

VERSION	DATE
3	2011-11-18

AUTHOR(S)
René Wugt Larsen,
University of Copenhagen

CLIENT(S)	CLIENT'S REF.
CCM	Marianne Jensen

PROJECT NO.	NUMBER OF PAGES/APPENDICES:
801820	25/ 4

ABSTRACT

Abstract
The photochemical degradation of nitrosamines in the troposphere is assessed with an aim to determine the lifetimes of these important compounds. The photolysis frequency of compounds in the atmosphere depends on the absorption cross sections of the molecules and the available sunlight. The cross sections (UV spectra) can be determined experimentally by measuring the UV spectrum of the compounds and theoretically by quantum chemical methods. Both methods were employed in this study. Experimental determination of the UV spectrum was successful for diethylnitrosamine, but impossible for other nitrosamines due to the low vapour pressures of these compounds. The absorption cross sections for a number of nitrosamines were determined theoretically with good agreement with known experimental data. The photolysis frequencies were calculated using the cross sections and the solar flux for different scenarios and the data confirmed that nitrosamines are photolyzed rapidly. By comparison with OH reaction it is shown that photolysis is the dominant gas phase removal process at all times of year. When there is insufficient radiation to remove the compounds by photolysis and radical concentrations are likewise low, removal by deposition will be key. This is estimated to be the case from November to February. While there is potentially a risk of higher nitrosamine concentrations during the three darkest months of the year, overall these compounds are removed rapidly from the gas phase. In conditions of very high NOx, conversion of nitrosamines to nitramines might need to be considered.

PREPARED BY	SIGNATURE
René Wugt Larsen	*René Wugt Larsen*

CHECKED BY	SIGNATURE
Torbjørn Pettersen / Eirik Falck da Silva	

APPROVED BY	SIGNATURE
Ole Wærnes, Research Director	

REPORT NO.	ISBN	CLASSIFICATION	CLASSIFICATION THIS PAGE
SINTEF F21202	ISBN	Confidential	Confidential

SINTEF

Document history

VERSION	DATE	VERSION DESCRIPTION
3	2011-11-18	Revised in accordance with comments sheet received 2011-10-26, and merged with SINTEF Report Template
2	2011-10-10	Revised in accordance with comments sheet received 2011-09-08
1	2011-08-16	First draft

PROJECT NO.
60120

REPORT NO.
SINTEF 2020

VERSION
3

2 of 30

Table of contents

SINTEF

1 Executive Summary

The photochemical degradation of nitrosamines in the troposphere is assessed with an aim to determine the lifetimes of these important compounds. The photolysis frequency of compounds in the atmosphere depends on the absorption cross sections of the molecules and the available sunlight. The cross sections (UV spectra) can be determined experimentally by measuring the UV spectrum of the compounds and theoretically by quantum chemical methods. Both methods were employed in this study. Experimental determination of the UV spectrum was successful for diethylnitrosamine, but impossible for other nitrosamines due to the low vapour pressures of these compounds. The absorption cross sections for a number of nitrosamines were determined theoretically with good agreement with known experimental data. The photolysis frequencies were calculated using the cross sections and the solar flux for different scenarios and the data confirmed that nitrosamines are photolyzed rapidly. By comparison with OH reaction it is shown that photolysis is the dominant gas phase removal process at all times of year. When there is insufficient radiation to remove the compounds by photolysis and radical concentrations are likewise low, removal by deposition will be key. This is estimated to be the case from November to February. While there is potentially a risk of higher nitrosamine concentrations during the three darkest months of the year, overall these compounds are removed rapidly from the gas phase. In conditions of very high NO_x, conversion of nitrosamines to nitramines might need to be considered.

2 Nitrosamine Photolysis in the Troposphere

2.1 Overview

Solar ultraviolet radiation is the driving force for tropospheric photochemical processes. Photons with ultraviolet wavelengths have sufficient energy to dissociate even fairly stable molecules into very reactive fragments by photolysis and thus initiate chemical reactions. The atmospheric oxidation of trace compounds is initiated by the photolytic production of radicals and reactive species such as the hydroxyl radical, nitrate radical, nitric oxide and ozone. Some of the process and atmospheric degradation products of amine-based carbon capture and storage can potentially be photolyzed in the atmosphere. In particular, nitrosamines and nitramines which may be formed as degradation products pose particular risks to human health. The NNO group of nitrosamines acts as a strong chromophore i. e. this functional group enables the nitrosamines to absorb ultraviolet radiation. The absorption of ultraviolet photons leads to rapid breaking of the N-NO bonds with a quantum yield of 1 owing to the anti-bonding character of the exited electronic states of the nitrosamine. The photolysis rate for this removal process thus depends both on the electronic excitation energies and corresponding absorption cross section of a given nitrosamine and the availability of solar ultraviolet radiation with corresponding wavelengths in the environment at the Mongstad location.

2.2 Photolysis Mechanisms
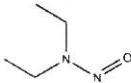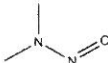
The importance of photolysis as a removal process for amine degradation products was initially considered in the H&ETQP Amine 4 Report. Ultraviolet transitions for a molecule correspond to electronic excitations between the energy levels that correspond to the molecular orbitals of the system. In particular, transitions involving p orbitals and lone pairs are relevant for the range of radiation available in the troposphere. The unit of the molecule that is responsible for the absorption is called the chromophore, of which the most common are C=C (π to π^*) and C=O, N, S (n to π^*) systems. Aliphatic compounds can usually only

undergo $\sigma \rightarrow \sigma^*$ transitions, and compounds with non-bonding electrons such as amines can undergo $n \rightarrow \sigma^*$ transitions. Both kinds of transitions require higher energies and hence shorter wavelengths (< 250 nm) than are available in the troposphere. These compounds therefore do not photolyze to a significant degree. Tropospheric photolysis of organic compounds is thus based on transitions of n or π electrons to the π^* excited state which generally occur at longer wavelengths (> 300 nm). These transitions occur in unsaturated compounds such as alkenes and also in nitrosamines and nitramines, making these potential candidates for photolysis under tropospheric conditions.
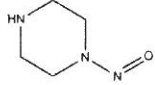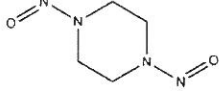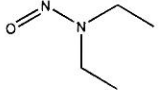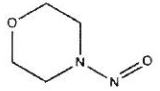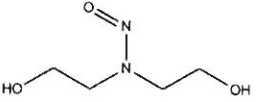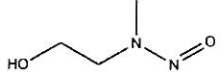
2.3 Degradation Products

The four generic amines are piperazine, 2-amino-2-methylpropanol (AMP), 2-ethanolamine (MEA) and N-methyldiethanolamine (MDEA). These are all saturated compounds and as such are not expected to photolyze significantly in the troposphere. On the other hand, some of the degradation products such as aldehydes and particularly nitrosamines are expected to undergo photolysis. The UV absorption cross sections for common aldehydes e. g. formaldehyde and acetaldehyde are well determined. A number of nitrosamines and nitramines have been identified as degradation products of these four generic amines. These compounds are known to be carcinogenic, and their atmospheric residence times need to be determined for risk assessment. These compounds are potential candidates for photolysis under tropospheric conditions due to the NO and NO_2 functional groups. However, preliminary theoretical predictions of the UV absorption spectra carried out for the H&ETQP Amine 4 project indicated that nitramines in general do not exhibit absorption features above 300 nm, where there is solar radiation available in the troposphere. These compounds are therefore very long-lived with respect to UV photolysis (lifetimes of more than 100 hours during summer) and the removal of these compounds will be dominated by other processes. The preliminary calculations showed that most nitrosamines have $n \rightarrow \pi^*$ absorption bands in the spectral region between 300 and 400 nm which makes photolysis a potentially important removal process for these compounds. It is thus important to quantify the UV cross sections of nitrosamines as accurately as possible by both experiment and using extensive theoretical methodologies to assess the importance of photolysis relative to the other removal processes. The six target nitrosamine compounds being investigated in this work are N-nitrosodimethylamine, 1-nitrosopiperazine, 4-nitrosomorpholine, 1,4-dinitrosopipera-zine, N-nitrosodiethanolamine and 2-(methylnitrosoamino)-ethanol labelled A to F in Table 1.

Table 1: *Structures and vapor pressures at 298 K for the target nitrosamines.*

Name	CAS	Structure	Vapor Pressure / hPa (298K)
N-nitrosodiethylamine	55-18-5		2.3
N-nitrosodimethylamine (A)	62-75-9		6.1

1-nitrosopiperazine (B)	5632-47-3		$2 \cdot 10^{-2}$
1,4-dinitrosopiperazine (C)	140-79-4		$3 \cdot 10^{-6}$
N-nitrosodiethyl amine	55-18-5		7.6
4-nitrosomorpholine (D)	59-89-2		0.15
N-nitrosodiethanolamine (E)	1116-54-7		$5 \cdot 10^{-7}$
2-(methylnitrosoamino) ethanol (F)	26921-68-6		$7 \cdot 10^{-4}$

2.4 Literature Summary

UV spectral data for the target nitrosamines are only available in the literature for N-nitrosodimethylamine and the photolysis of this compound has been investigated in the gas phase by Bamford, Lindley & Calvert[1], Tuazon et al.[2] and Geiger & Huber[3]. In addition, Stefan and Bolton[4] studied the photolysis of this compound in aqueous solutions at two different pH values and identified CH_3NH_2, HCHO, HCOOH, N_2O, $(CH_3)_2NH$ and $CH_2=NCH_3$ as the main products. Tuazon et al.[2] extracted the photolysis rate relative to that of NO_2 to be $j_{NDMA} / j_{NO2} = 0.53 \pm 0.03$. The fast photolysis corresponds to a quantum yield value of 1 around 290 nm in agreement with the value of 1.03 ± 0.10 reported by Geiger & Huber[3] at 363.5 nm. These results indicate that nitrosamine photolysis lifetimes are in the order of minutes under tropospheric conditions and photolysis should be considered as an important removal process.

3 Specification of Summer, Winter and Equinox Conditions

3.1 The Solar Actinic Flux

The photolysis rate of a compound in the troposphere depends both on the spectroscopic properties of the molecule and the amount of solar radiation available. Since the Mongstad facility is located at high latitude, the flux of solar radiation varies significantly throughout the year. It is therefore not sufficient to simply consider the annual average conditions to evaluate the contribution from photolysis and extreme scenarios (summer, winter and equinox) have to be evaluated individually. It is important to consider both the photolysis lifetime at the maximum radiation levels during the summer and the minimum levels during the winter. Photolysis is potentially an important removal process in summer but less important in winter, at which time other removal channels have to be considered. In addition, the penetration of solar radiation in

the atmosphere below 1000 nm is predominantly determined by the absorption of oxygen and ozone and scattering by clouds. The amount of ultraviolet radiation penetrating the troposphere therefore depends slightly on the actual ozone column. The Hartley absorption band of ozone effectively prevents radiation with wavelengths shorter than 300 nm from reaching the troposphere.

3.2   Tropospheric Ultraviolet and Visible Radiation Model

The solar spectral actinic flux for the geographical location of the Mongstad plant (60.8°N; 5.03°E) has been generated by the Tropospheric Ultraviolet and Visible (TUV) Radiation Model version 4.1 provided by National Centre for Atmospheric Research (NCAR)[5]. This radiation model provides solar actinic flux spectral data for specified latitude, longitude and a specific time at a given altitude above the surface. In addition, the effect of surface albedo and the total ozone column can be considered. At standard conditions the ozone column has an average value of around 300 Dobson units. This value is used in all the scenarios considered in the present work.
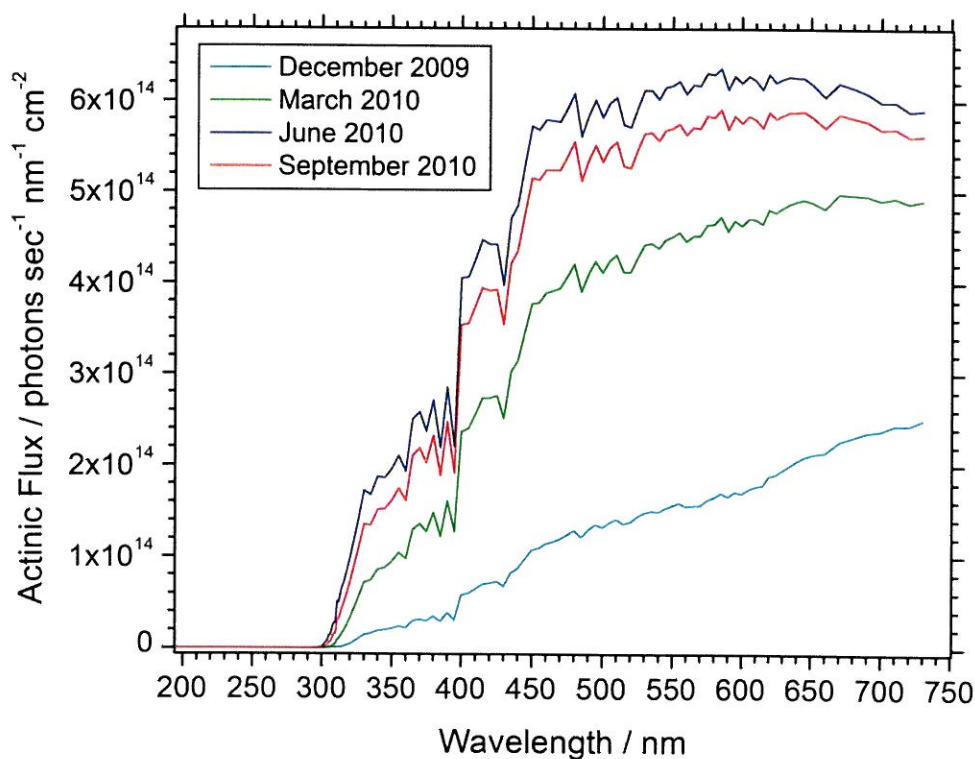
Figure 1: *The observed seasonal variation of the midday solar actinic flux at an altitude of 0.5 km for the local Mongstad environment (60.8° N; 5.03° E).*

3.3 Seasonal Actinic Solar Flux Data for the Mongstad Location

Fig. 1 shows the midday solar actinic flux in the ultraviolet and visible regions of the electromagnetic spectrum for winter (December 2009), summer (June 2010) and the equinox conditions during March 2010 and September 2010. Fig. 2 shows the solar spectral actinic flux curves for the different altitudes 0.5, 2, 4, 6 and 8 km above the Earth's surface at the environment for the Mongstad location at the time of the seasonal minimum in December. The extracted data at the location of the Mongstad facility show that the midday solar flux is at least an order of magnitude smaller during the winter relative to the summer season depending on the exact wavelength region. In addition, the solar flux on average is a factor of 2 to 3 smaller close to the Earth's surface relative to the value observed at an altitude of 8 km close to the tropopause at this latitude. At winter solstice (December 22), the sun rises around 9:00 am local time at the Mongstad location and stays very low above the horizon until it sets again around 3:30 pm local time. In Appendix A, we have examined the daily variation of the actinic solar flux during daytime to assess the role of photolysis as removal process around winter solstice.
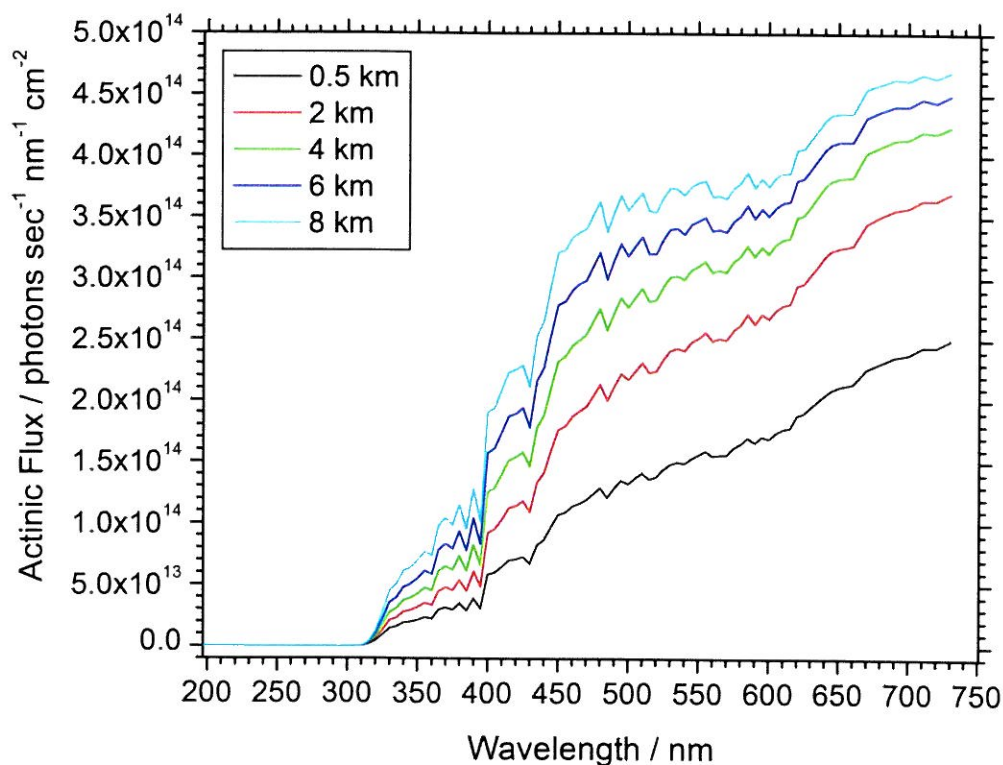
Figure 2: *The altitude variation (0.5, 2, 4, 6 and 8 km) of the midday solar actinic flux for the local Mongstad environment (60.8° N; 5.03° E) observed for December 2009.*

4 UV-VIS Absorption Spectra: Experiment and Theory

Ultimately, highly accurate experimental UV-VIS absorption spectra of the six target nitrosamines would provide the most reliable estimates of their lifetimes with respect to photolysis in the troposphere. However, most of the target nitrosamines have extremely low vapour pressures at ambient temperatures (Table 2) and such quantitative experimental studies are demanding. For the most volatile of the nitrosamines, N-nitrosodimethylamine, electronic spectral data already exist in the literature. In order to extend this limited set of experimental data in the literature, the UV-VIS absorption spectrum for another volatile compound in this class of compounds, N-nitrosodiethylamine, has been recorded. Extensive complementary quantum chemical spectral predictions have been carried out for all the target compounds including N-nitrosodiethylamine. As shown below the direct comparison between the available experimental spectral data and predictions from a variety of theoretical methodologies indicate the level of theory required to obtain reliable UV-VIS cross sections for the determination of nitrosamine photolysis rates.

4.1 Fourier Transform UV-VIS Absorption Spectroscopy

4.1.1 Data Acquisition

The electronic absorption spectra of the N-nitrosodiethylamine samples were collected employing the Bruker IFS 66v/S vacuum Fourier transform interferometer located at the Copenhagen Centre for Atmospheric Research (CCAR) which is suitable for absorption spectroscopy in the spectral range from the IR and VIS to the VUV spectral region[6]. The Fourier transform interferometer was equipped with a UV/VIS quartz beam splitter, broadband UV radiation was generated by a stabilized Deuterium discharge lamp through a 1 mm aperture and the modulated signals were monitored by a GaP-diode detector.

Single-beam spectra of the backgrounds and samples were generated from an average of 500 interferograms collected with a spectral resolution ranging from 25 to 50 cm^{-1} (total scan times of 4-5 min, respectively) employing a Blackman-Harris three-term apodization function and a zero-filling factor of two. The short scan times minimize both the effect of baseline drifting in the single-beam spectra and the degree of sample adsorption and thereby enable the determination of more reliable absolute absorption cross sections. A series of background spectra were collected before and after each sample spectrum to further minimize the effect of baseline variations in the resulting transmittance spectra. The transmittance spectra have been generated from the ratio between the sample and the background single-beam spectra.

According to the Beer-Lambert law, the absorption cross section σ at a specific wavenumber ν ($\nu = 1/\lambda$ where λ is the wavelength) is given by:

$$\sigma(\nu) = \frac{A}{nL}$$

$A = -\log T(\nu)$ is the absorbance, $T(\nu)$ is the transmittance, n is the amount of compound and L is the optical length of the absorption path. The convention is to use the oscillator strength f to express the total strength of an electronic transition. In order to compare with theoretical predicted oscillator strength values we extract the total experimental absorption cross section $\int \sigma(\nu)d\nu$ by integrating over the full band profiles as a measure of the total absorption intensity. The relation between the integrated molar absorption cross section and the dimensionless oscillator strength f is given by:

$$f = 1.44 \times 10^{-19} \int \sigma(\nu)\,d\nu$$

In the field of UV-VIS absorption spectroscopy the convention is usually to employ the molar extinction coefficient, $\varepsilon(\nu) = \sigma(\nu)\,N_A$, where N_A is the Avogadro constant.

4.1.2 Sample Handling

Samples of N-nitrosodiethylamine with partial pressures in the range from 0.2 to 0.8 hPa were kept in a 10 cm absorption gas cell equipped with CaF_2 windows at 296 K. The handling of the nitrosamine samples followed the safe job analysis and HSE activities in the experimental plan accepted by Carbon Capture Mongstad. The container of the purchased N-nitrosodiethylamine sample (≥ 99.0% (GC), Sigma Aldrich®) was sealed with a septum. Small portions of this sample were transferred to a sample container via a syringe in a fume hood. The sample container was mounted to a gas-handling system equipped with a calibrated 0-10 Torr range pressure gauge, a cold trap protected vacuum pump and the employed absorption cell. The handling of the N-nitrosodiethylamine samples involved the use of protection gloves and full-face respirators with installed multi-purpose combination respirator cartridges designed for nitrosamines. N-nitrosodiethylamine is extremely prone to cell wall adsorption and it was therefore hard to monitor the decreasing sample pressures better than 3-5% accuracy.

4.1.3 Experimental Results and Errors

Fig. 3 shows the UV-VIS absorbance cross section of N-nitrosodiethylamine recorded with rather low sample pressures where the overlap between the weak $n \rightarrow \pi^*$ transition and the higher energy electronic transitions are limited. The accuracy of the observed $n \rightarrow \pi^*$ band origin is basically determined by the spectral resolution and we estimate a band origin of 368.5 ± 0.5 nm. This value is very close to the observed band origin of 363.5 nm reported for N-nitrosodimethylamine by Geiger et al.[3] and supports that the class of nitrosamines in general possesses a characteristic $n \rightarrow \pi^*$ chromophore with band centres around 365 nm.
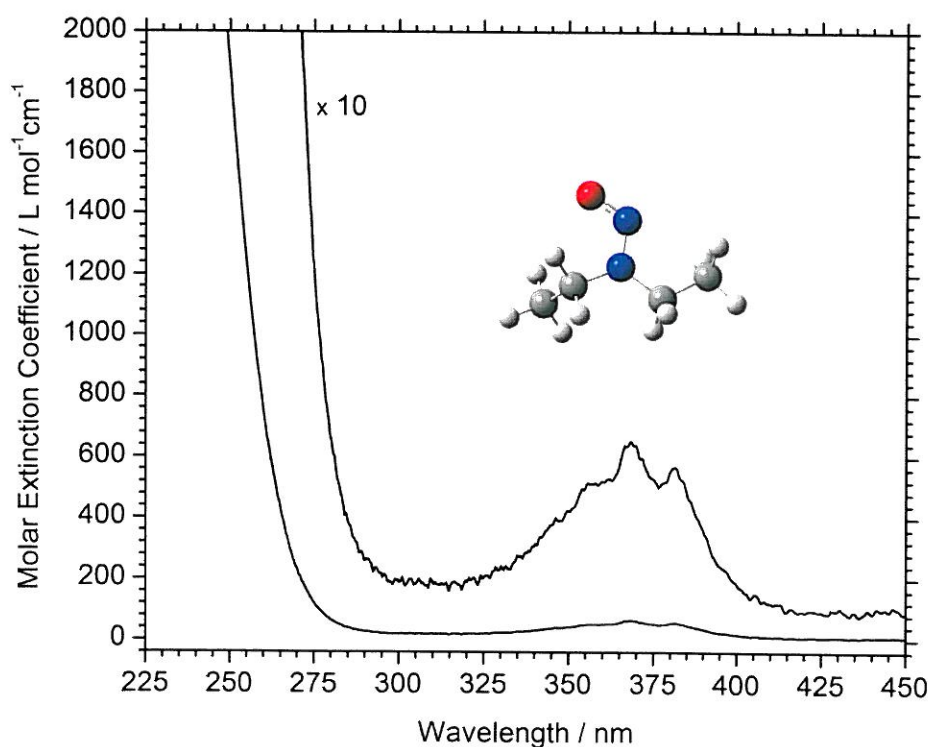
Figure 3: Experimental UV-VIS absorption spectrum for N-nitrosodiethylamine recorded at 296 K by the Bruker IFS66v/S vacuum Fourier transform spectrometer.

The major experimental error sources for the extracted absorption cross sections are the monitored sample pressures (ca. 3-5%), the optical path length of the absorption cell (ca. 1%), the sample temperature (ca. 1%) and baseline drifting in the single-beam spectra (ca. 1%). The error propagation thus indicates overall expected standard deviations in the order of ca. 5-7% for the experimental UV cross sections.

At sample pressures above ca. 0.5 hPa, the overlap between the weak $n \rightarrow \pi^*$ transition and the much stronger electronic transitions at higher energies precludes reliable integration over the complete band profile to extract a value for the total integrated extinction coefficient or oscillator strength to compare with the theoretical predictions. The UV-VIS absorption spectra recorded with sample pressures less than 0.5 hPa do not have severely overlapped band profiles and we are able to estimate a value for the dimensionless oscillator strength $f = 0.00065 \pm 0.00005$ for the $n \rightarrow \pi^*$ transition based on the low pressure measurements.

4.2 Quantum Chemical Predictions of Electronic Transitions

3.2.1 Time-Dependent Density Functional Theory

It is generally agreed that time-dependent density functional theory (TD-DFT) is a promising methodology for reliably predicting electronic spectra. DFT calculations are less expensive in terms of CPU time, memory, and disk space than the benchmark coupled cluster methodologies since the DFT approaches are based on total electron densities rather than wave functions. In particular, the B3LYP functional has been shown to provide reliable UV-VIS absorption spectra for several classes of medium-sized organic molecules[7]. In the present assessment, we explore the ability of three different TD-DFT approaches (B3LYP, B2PLYPD and BP86) to predict reliable electronic spectra for the class of nitrosamines.

3.2.2. Coupled Cluster Approach

The benchmark coupled cluster approach provides a hierarchy of methods denoted CCS, CC2, CCSD, CC3, CCSDT including electronic correlation. The accuracy is improved via the cluster expansion from singles S, through singles and doubles SD, to singles, doubles and triples SDT, etc. and the computational cost increases significantly with the cluster expansion. In this work, we have focused solely on the CCSD level which is the generally applicable method for medium sized molecular systems[8].

3.2.2 Theoretical Results: Dependence on Basis Set and Methodology

Since N-nitrosodimethylamine is the smallest of the six target compounds, a direct comparison between experimental spectral data and high-level coupled cluster methods is feasible for this compound. The CCSD prediction of the equilibrium configuration of N-nitrosodimethylamine employing the triple zeta basis set cc-pVTZ (the most demanding level of theory employed in the present work) required 340 hours of CPU time. The prediction of excitation energies and oscillator strengths for the five lowest electronic transitions required an additional 190 hours of CPU time. The quantum chemical calculations have been computed on desktop facilities at the University of Copenhagen and using the STENO cluster at DCSC (Danish Centre for Scientific Computing at Copenhagen University) employing the Gaussian 09 suite of programs[9]. Table 2 shows the results from a basis set analysis of the excitation wavelength and corresponding oscillator strength for the relevant $n \rightarrow \pi^*$ transition for N-nitrosodimethylamine predicted by the TD-DFT approach

employing the B3LYP functional. The series of Dunnning basis sets (aug)-cc-pVNZ where N = D (double), T (triple), Q (quadruple) both with and without extra primitive diffuse functions (denoted aug) have been tested.

Table 2: Basis set analysis of the excitation wavelength and corresponding oscillator strength for the relevant $n \rightarrow \pi^*$ transition of N-nitrosodimethylamine predicted by the TD-DFT approach employing the B3LYP model and Dunnning basis sets (aug)-cc-pVNZ (N = D, T and Q).

Level of Theory	Vertical Excitation Wavelength / nm	Oscillator Strength
B3LYP/cc-pVDZ	359.1	0.0012
B3LYP/cc-pVTZ	357.1	0.0011
B3LYP/cc-pVQZ	357.4	0.0010
B3LYP/aug-cc-pVDZ	361.4	0.0010
B3LYP/aug-cc-pVTZ	358.7	0.0010
B3LYP/aug-cc-pVQZ	358.5	0.0010
Experimental	*363.5[a]*	

[a]G. Geiger and J. R. Huber, *Helvetica Chimica Acta* **64**, 989-995 (1981)

It appears that even the smallest double zeta basis set cc-pVDZ provides reliable excitation energies compared to the experimental findings. The addition of primitive diffuse functions in the basis sets (aug) turns out to improve the reliability at limited additional computational cost. We therefore employ Dunning's augmented triple zeta basis set aug-cc-pVTZ in the comparison with the B2PLYPD and BP86 models since this basis set size is feasible for all target compounds.

Table 3: Vertical electronic excitation wavelength and corresponding oscillator strength for the relevant $n \rightarrow \pi^*$ transition of N-nitrosodimethylamine predicted by the different TD-DFT approaches B2PLYPD, BP3LYP and BP86 and the benchmark (EOM) CCSD methodology.

Level of Theory	Vertical Excitation Wavelength / nm	Oscillator Strength
B2PLYPD/aug-cc-pVTZ	356.4	0.0011
B3LYP/aug-cc-pVTZ	358.7	0.0010
BP86/aug-cc-pVTZ	361.9	0.0011
EOM-CCSD/cc-pVDZ	344.6	0.0014
EOM-CCSD/aug-cc-pVDZ	346.8	0.0010
EOM-CCSD/cc-pVTZ	342.9	0.0012
Experimental	*363.5[a]*	

[a]G. Geiger and J. R. Huber, *Helvetica Chimica Acta* **64**, 989-995 (1981)

It is observed that both the vertical excitation wavelength and the corresponding oscillator strength for the $n \rightarrow \pi^*$ transition of N-nitrosodimethylamine is almost exactly reproduced at the basis set limits by the three different TD-DFT methods and the CCSD approach (Table 3). The excitation

wavelength is predicted to within 2-6% and the corresponding oscillator strength to within 10-20%. The TD-DFT spectral predictions also reproduce the experimental band origin and the corresponding oscillator strength observed for N-nitrosodiethylamine well (Table 4).

Table 4: Vertical electronic excitation wavelength and corresponding oscillator strength for the relevant n → π transition of N-nitrosodiethylamine predicted by three TD-DFT approaches and the benchmark Dunning basis set aug-cc-pVTZ.*

Level of Theory	Vertical Excitation Wavelength / nm	Oscillator Strength
B2PLYPD/aug-cc-pVTZ	359.1	0.0007
B3LYP/aug-cc-pVTZ	364.8	0.0006
BP86/aug-cc-pVTZ	372.7	0.0005
Experimental	*368.4[a]*	*0.00065[a]*

[a] This work

Since the CCSD approach is not feasible for systems with many electrons within the short timeframe of this assessment, we have chosen the widely used TD-DFT (B3LYP/aug-cc-pVTZ) approach for the spectral predictions of all six target nitrosamines (Table 5). In general, the predictions support the experimental findings that nitrosamines possess an organic $n \rightarrow \pi^*$ chromophore centered around 365 nm with corresponding oscillator strengths in the range from 0.0006 to 0.0011. As this approach has worked well for the range of nitrosamines in this study, we recommend that any new nitrosamines can be assessed using this level of theory. It should be noted that 1,4-dinitrosopiperazine contains two almost degenerate $n \rightarrow \pi^*$ transitions and the value of the total absorption cross section is a factor of two higher.

Table 5: Vertical electronic excitation wavelength and corresponding oscillator strength for the relevant n → π transition of the six target nitrosamines and N-nitrosodiethylamine predicted by the TD-DFT approach (B3LYP/aug-cc-pVTZ).*

Level of Theory	Vertical Excitation Wavelength / nm	Oscillator Strength
N-nitrosodiethylamine	364.8	0.0006
N-nitrosodimethylamine (A)	358.7	0.0010
1-nitrosopiperazine (B)	362.8	0.0008
1,4-dinitrosopiperazine (C)	362.5	0.0016
4-nitrosomorpholine (D)	363.0	0.0008
N-nitrosodiethanolamine (E)	366.0	0.0009
2-(methylnitrosoamino) (F) ethanol	361.9	0.0011

5 Determination of Photolysis Frequencies and Mean Lifetimes

5.1 Simulation of Total Molar Extinction Coefficients

In order to relate the absorption cross sections to tropospheric photolysis rates, the first step is to convert the predicted transition energies and corresponding oscillator strengths into actual UV absorption spectra by simulating the vibrational progressions and overlaps between the different electronic transitions. This has been done with the GaussView 5.0 program package (Gaussian, Inc.) where the molar extinction coefficients have been obtained by convoluting the predicted line functions with Gaussians defined by the band origins (excitation energies), total integrated intensities (oscillator strengths) and half-widths employing the default values of GaussView 5.0. The simulation of the total molar extinction coefficient versus wavelength is thus generated by the superposition of the individual Gaussian profiles.

The total molar extinction coefficients versus wavelength for N-nitrosodimethylamine simulated for the different TD-DFT approaches are illustrated in Fig. 4. The three simulated UV-VIS absorption spectra are almost identical although the overlap with the stronger electronic transitions at higher energy is overestimated by the BP86 model for the critical spectral region around 300 nm. It should be noted that the stronger overlap predicted by the BP86 model does not alter the calculated value of the final photolysis frequency for N-nitrosodimethylamine by more than 10% (see section 4.2).
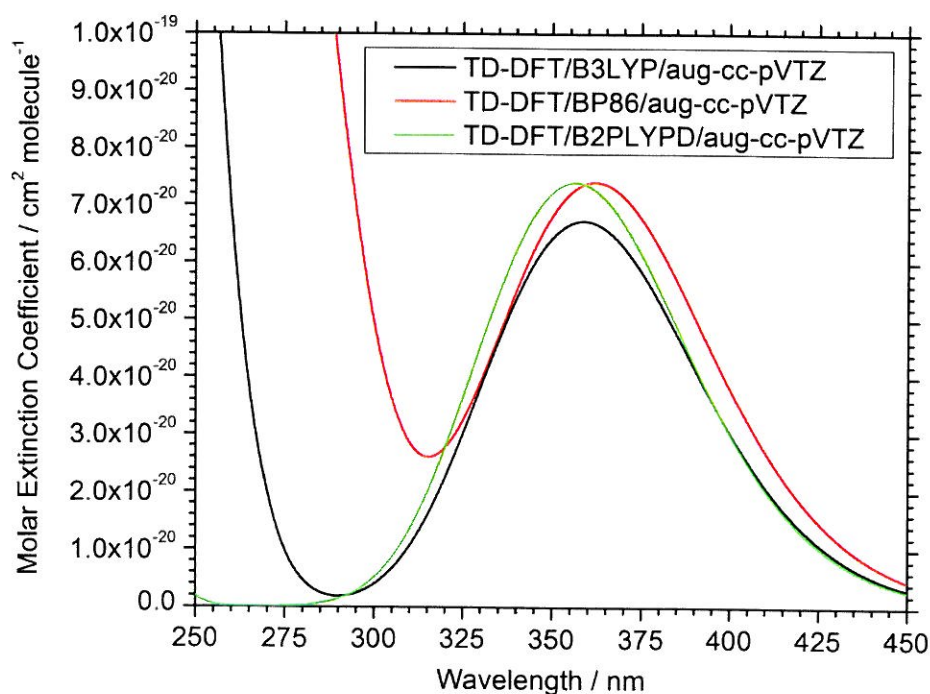
Figure 4: Simulations of the TD-DFT (B3LYP, BP86 and B2PLYPD) predictions of the total molar extinction coefficient (cm^2 molecule^{-1}) versus wavelength for N-nitrosodimethylamine in the spectral region relevant for tropospheric photolysis.

5.2 Integration of Solar Flux Overlap Region

The simulated UV absorption spectra for the target nitrosamines predicted by the TD-DFT B3LYP/aug-cc-pVTZ calculations have been employed to determine the tropospheric photolysis frequencies and mean

lifetimes with respect to photolysis. The photolysis frequency, the *J*-value, is given by the following expression:

$$J = \int I(v)\Phi(v)\sigma(v)\,dv$$

where $I(v)$ is the solar actinic flux at a given time of the year (units of photons $s^{-1}\,nm^{-1}\,cm^{-2}$) and $\sigma(v)$ is the predicted molar extinction coefficient (units of $cm^2\,molecule^{-1}$) of the target compound at the wavelength v (units of nm). The quantum yield $\Phi(v)$ is assumed to be 1, an assumption which is both supported by the experimentally determined value of 1.03 ± 0.10 reported for N-nitrosodimethylamine by Geiger & Huber[3] and another study by Tuazon *et al.*[2] For a given radiation field, the *J*-value describes the first order rate of photolysis of the nitrosamine. The *J*-value depends therefore on the local solar radiation field which varies with the latitude, longitude and time at a given altitude above the surface. As for any first-order decay reaction, the reciprocal *J*-value gives the mean photolysis lifetime τ of the nitrosamine:

$$\tau_{photolysis} = \frac{1}{J}$$

Fig. 5 shows the overlap region of the simulated UV absorption spectrum of N-nitrosodimethyl-amine (B3LYP/aug-cc-pVTZ level of theory) and the solar actinic flux curve for June 2010. It appears that the electronic transition $n \rightarrow \pi^*$ around 363.5 nm has a strong overlap with the actinic flux curve resulting in rather short photolysis lifetimes of nitrosamines with respect to photolysis in the troposphere. The detailed overlap region versus wavelength shown in Appendix C illustrates that the UV-B cut-off around 300 nm for the solar actinic flux curve defines the high-energy limit of the overlap regions. This is the reason why the stronger electronic transition at shorter wavelengths does not affect the photolysis rates significantly. It should be noted that this very steep UV-B cut-off also is the reason why the class of nitramines in general are very long-lived with respect to photolysis. This class of compounds do not exhibit any absorption features at wavelengths longer than 300 nm. The mean photolysis lifetimes of the nitramines are thus several orders of magnitude larger than for nitrosamines and removal processes other than photolysis should be considered for the nitramines.

In order to investigate the dependence of the photolysis frequencies and corresponding mean photolysis lifetimes on the season, time of the day and the exact altitude in the troposphere we have calculated the overlap integrals between the simulated molar UV-VIS absorption spectra and the solar actinic flux curves at the different conditions. Numerical integration of the overlapping spectral regions between ca. 300 to 500 nm (Appendix C) has been carried out using Origin Pro 8.0 SR4 package (Origin Lab Corporation). The resulting values of the photolysis frequencies and corresponding mean photolysis lifetimes are listed in Table 6. Based on the combined experimental and theoretical results for N-nitrosodimethylamine and N-nitrosodiethylamine, we estimate the standard deviation to be on the order of 10-20% for the calculated values of the photolysis frequencies
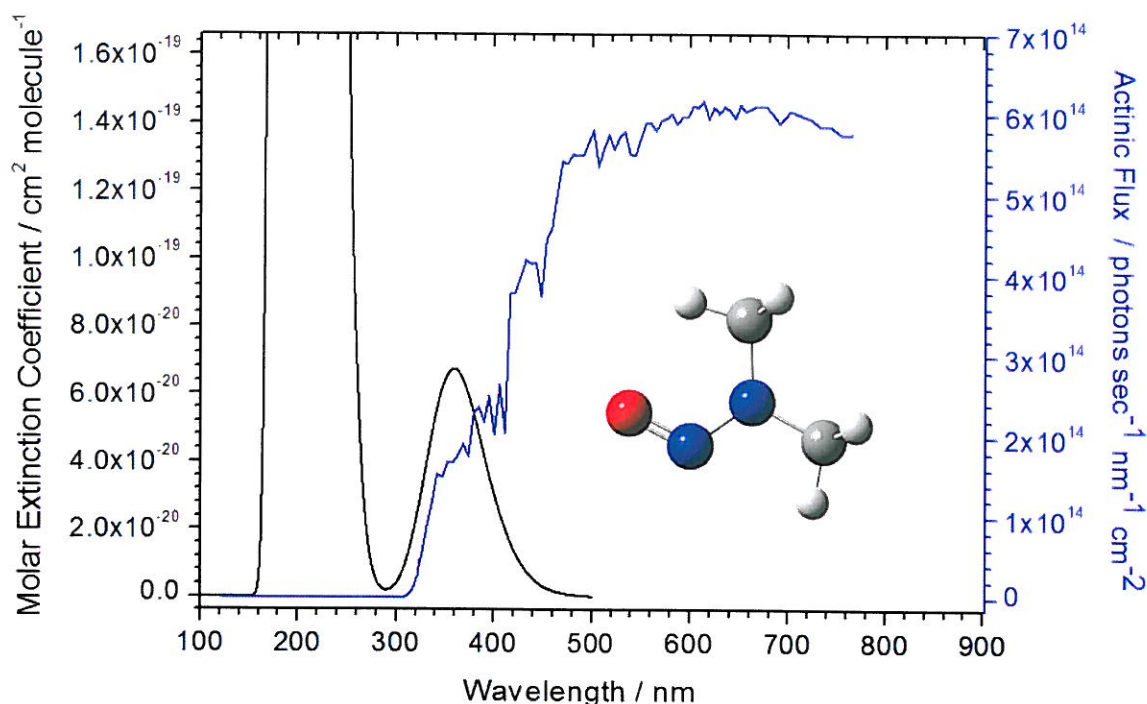
Figure 5: *The overlap region of the simulated UV absorption spectrum of N-nitrosodimethyl-amine (B3LYP/aug-cc-PVTZ level of theory) and the solar actinic flux curve (June 2010).*

We observe that for a given solar actinic flux the photolysis frequencies are almost identical for all six target nitrosamines owing to the characteristic $n \to \pi^*$ chromophore for this class of compounds. The photolysis frequency for 1,4-dinitrosopiperazine is almost twice as high owing to two almost degenerate $n \to \pi^*$ transitions. The variation of the photolysis frequency with altitude for N-nitrosodimethylamine listed in Table 6 is therefore also valid for the other five target nitrosamines. The photolysis constant is given relative to NO_2 ($J/J(NO_2)$) using NO_2 data from the NCAR TUV model. Photolysis constants are often obtained by scaling relative to NO_2, however it is important to note that the $J/J(NO_2)$ ratio depends on the solar flux and thereby on the latitude. This dependence arises because the UV spectra of NO_2 and the other compound do not overlap exactly.

Table 6: *The calculated photolysis frequency J and mean photolysis lifetime τ for the six target nitrosamines based on the simulated UV absorption spectra (B3LYP/aug-cc-pVTZ) and extracted solar actinic flux data for the Mongstad location at different times of the year (midday) and altitude above ground level (km).*

Time / Altitude / km	Photolysis Frequency J / s^{-1}	$J/J(NO_2)$	Mean Photolysis Lifetime τ / hour
N-nitrosodimethylamine (A)			
September 2010 / 0.5	1.0×10^{-3}	0.14	0.28
June 2010 / 0.5	1.2×10^{-3}	0.13	0.23

PROJECT NO.
SINTEF

REPORT NO.
SINTEF F21702

VERSION

17 of 30

Time / Altitude / km	Photolysis Frequency J / s^{-1}	$J/J(NO_2)$	Photolysis Lifetime τ / hour
March 2010 / 0.5	6.5×10^{-4}	0.11	0.43
December 2009 / 0.5	1.5×10^{-4}	0.17	1.85
/ 2	2.4×10^{-4}	0.19	1.16
/ 4	3.2×10^{-4}	0.18	0.86
/ 6	4.1×10^{-4}	0.18	0.68
/ 8	5.0×10^{-4}	0.17	0.56
1-nitrosopiperazine (B)			
September 2010 / 0.5	8.9×10^{-4}	0.13	0.31
June 2010 / 0.5	1.0×10^{-3}	0.11	0.26
March 2010 / 0.5	5.7×10^{-4}	0.09	0.49
December 2009 / 0.5	1.4×10^{-4}	0.16	2.03
1,4-dinitrosopiperazine (C)			
September 2010 / 0.5	1.8×10^{-3}	0.26	0.16
June 2010 / 0.5	1.9×10^{-3}	0.20	0.15
March 2010 / 0.5	1.1×10^{-3}	0.18	0.25
December 2009 / 0.5	2.7×10^{-4}	0.31	1.02
4-nitrosomorpholine (D)			
September 2010 / 0.5	8.9×10^{-4}	0.13	0.31
June 2010 / 0.5	1.1×10^{-3}	0.12	0.26
March 2010 / 0.5	5.9×10^{-4}	0.10	0.49
December 2009 / 0.5	1.5×10^{-4}	0.17	2.02

Table 5: Continued

Time / Altitude / km	Photolysis Frequency J / s^{-1}	$J/J(NO_2)$	Photolysis Lifetime τ / hour
N-nitrosodiethanolamine (E)			
September 2010 / 0.5	1.1×10^{-3}	0.16	0.26
June 2010 / 0.5	1.2×10^{-3}	0.13	0.22
March 2010 / 0.5	6.9×10^{-4}	0.11	0.40

PROJECT NO
SINTEF
REPORT NO
SINTEF F21762
VERSION
19 of 30

December 2009 / 0.5	1.7×10^{-4}	0.20	1.66
2-(methylnitrosoamino)- (F) ethanol			
September 2010 / 0.5	1.2×10^{-3}	0.17	0.23
June 2010 / 0.5	1.4×10^{-3}	0.15	0.20
March 2010 / 0.5	7.7×10^{-4}	0.13	0.36
December 2009 / 0.5	1.8×10^{-4}	0.21	1.51

6 Tropospheric Box Modelling

6.1 The Box Model

The predicted values of the photolysis frequencies for the six target nitrosamine have been implemented in a tropospheric box model using the Kintecus chemical kinetics simulation program[10]. The Kintecus simulation software includes a compiler to model the reactions of atmospheric chemical kinetic and equilibrium processes.[11] For the present purposes, the box model has been constructed to evaluate the removal of the six studied nitrosamines by photolysis and by reaction with hydroxyl radicals. Elements of this model can be incorporated in a larger scale meteorological model.

The model includes 169 chemical reactions, including the Ox, HOx, NOx and hydrocarbon chemistry that drives the concentration of reactive species in the atmosphere. The model includes methane, ethane, propane and isoprene as hydrocarbon species. All of these compounds react with the OH radical and the reactions with NO_3 and Cl radicals have also been incorporated. The reaction rate constants have been taken from the established kinetics databases (JPL Photochemical Database, IUPAC Gas Kinetic Data Evaluation)[12].

For the nitrosamines, the OH reaction rates are unknown except for N-nitrosodimethylamine for which the rate constant has been experimentally determined to be $3.0 \pm 0.4 \times 10^{-12}$ cm^3 molecule^{-1} s^{-1} at room temperature. For the other nitrosamines an alternative is to use OH reaction rate constants predicted by quantitative structure-activity relationship (QSAR) calculations employed by the EPI Suite™ [12]. However, since this QSAR approach is known to be inaccurate and likely overestimates the rate constants for amines and nitrosamines, we have chosen instead to use the experimental value for N-nitrosodimethylamine for all nitrosamines. The model scenarios have been carried out with a starting concentration of 5 ppt for each of the nitrosamines. Initial concentrations of other atmospheric species (hydrocarbons, H_2O, NO_x, etc.) have been taken from the literature[13].

6.2 Seasonal Variation of Nitrosamine Removal

Figures 6a - 6d show the change in concentration of the six nitrosamines during 3 hour runs of the box model at the four different seasons of the year (equinoxes and solstices, photolysis data at midday). The compounds are solely being removed by photolysis and the OH reaction. The runs show that during March, June and September the half-life of the nitrosamines is less than an hour and the compounds are completely removed in a matter of 2-3 hours.

The scenario for December differs significantly from the other seasons: the lifetime of the nitrosamines is almost an order of magnitude longer in December compared to June. With a half-life around three hours, the compounds cannot be expected to be completely removed by these processes during the darkest days of the

PROJECT NO.
SINTEF

REPORT NO.
SINTEF F21202

VERSION

19 of 30

year. Figures 7a - 7b show a scenario in June and December respectively where 1ppm dimethylamine has been emitted. Assuming a 100% conversion of DMA to dimethylnitrosamine, which is a worst-case scenario, it can be seen that in June the dimethylnitrosamine concentration is at a maximum after about one hour and then begins to drop. In winter the dimethylnitrosamine is still building up after two hours as there is not sufficient sunlight to remove it. In these scenarios the OH radical serves to break down the DMA, but the dimethylnitrosamine removal by OH is negligible compared to photolysis.
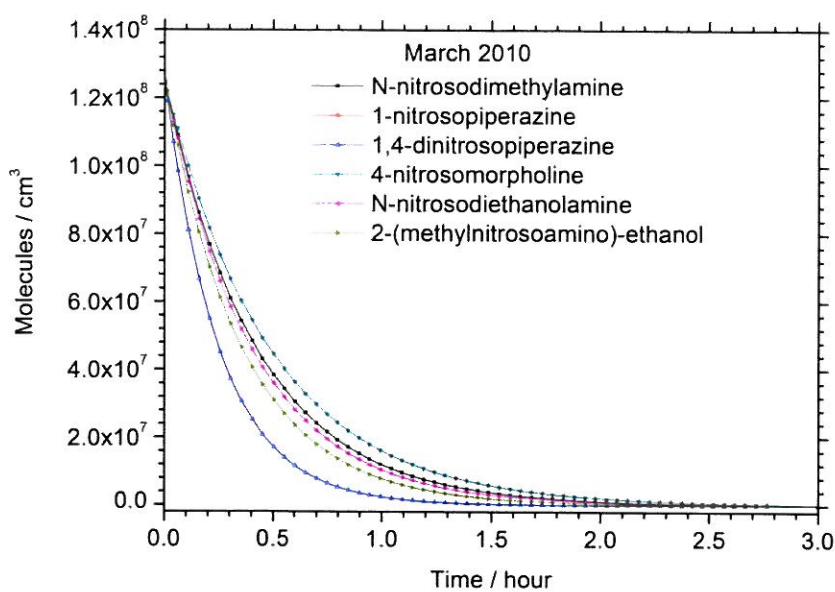
Figure 6a: The total fate of the six target nitrosamines at the Mongstad location (0.5 km altitude) midday March 2010 predicted by the one-dimensional tropospheric Kintecus box model.
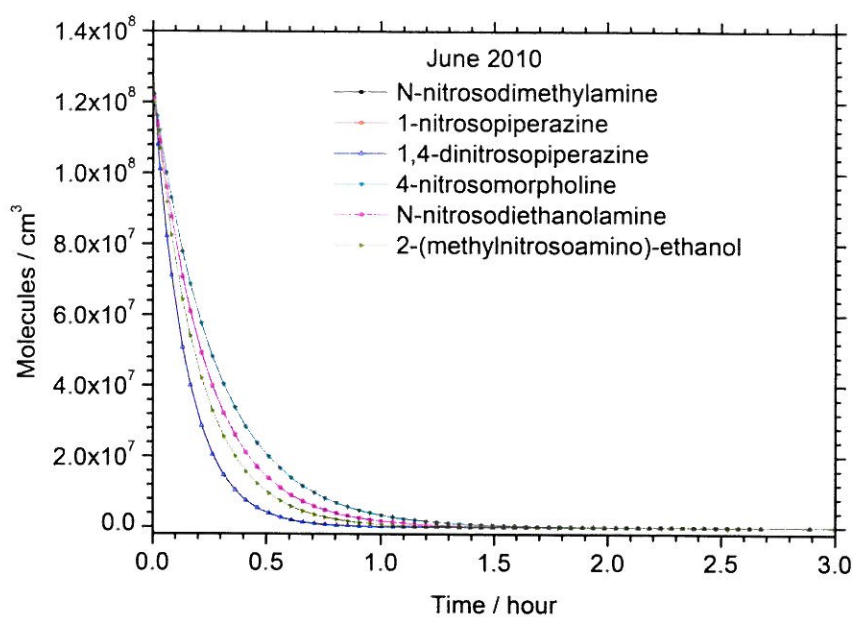
Figure 6b: The total fate of the six target nitrosamines at the Mongstad location (0.5 km altitude) midday June 2010 predicted by the one-dimensional tropospheric Kintecus box model.
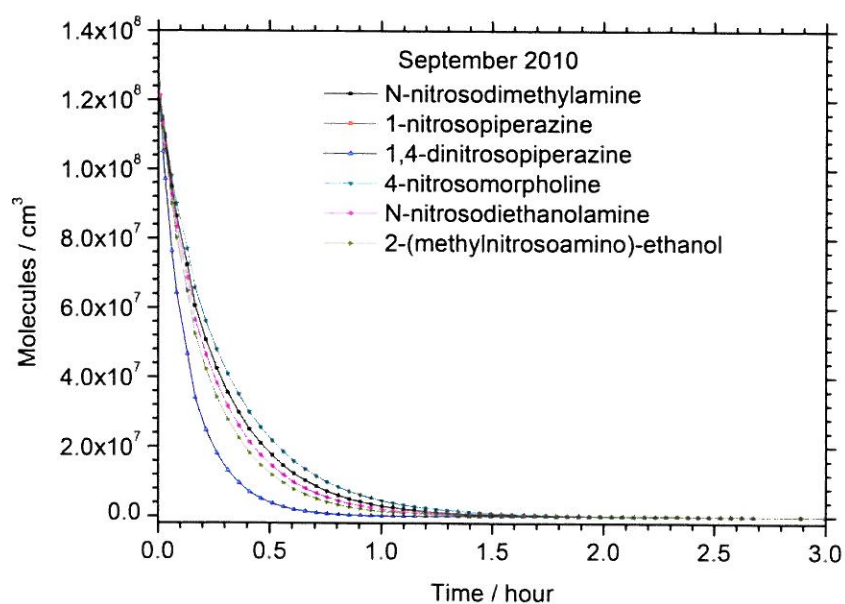

Figure 6c: The total fate of the six target nitrosamines at the Mongstad location (0.5 km altitude) midday September 2010 predicted by the one-dimensional tropospheric Kintecus box model.
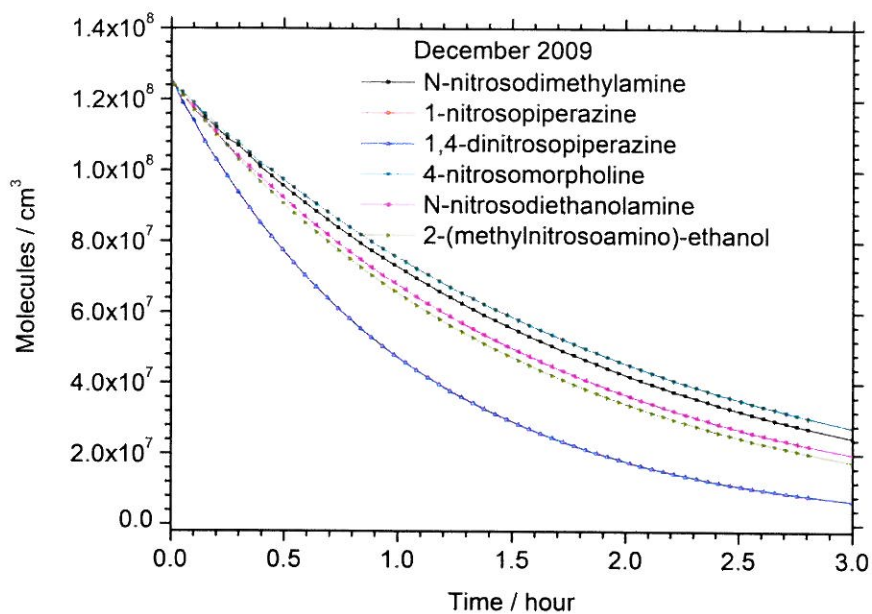
Figure 6d: The total fate of the six target nitrosamines at the Mongstad location (0.5 km altitude) midday December 2009 predicted by the one-dimensional tropospheric Kintecus box model.
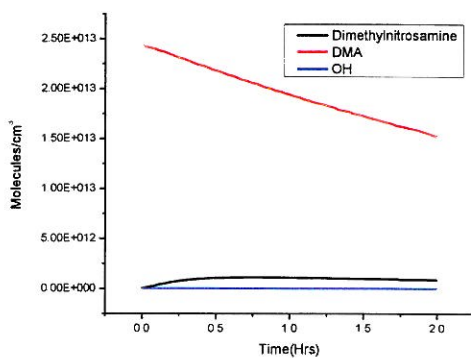

Figure 7a: Model scenario of nitrosamine formation after a 1ppm emission of dimethylamine in June at midday. The model assumes a 100% conversion of DMA to dimethylnitrosamine.
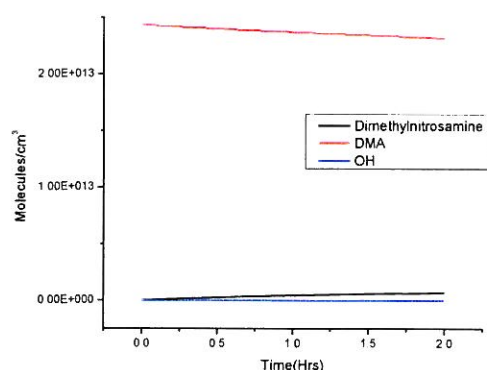
Figure 7b: Model scenario of nitrosamine formation after a 1ppm emission of dimethylamine in December at midday. The model assumes a 100% conversion of DMA to dimethylnitrosamine.

6.3   Photolysis versus Chemistry

Figure 8 shows two model scenarios in December where the nitrosamines are being removed by photolysis and the OH reaction exclusively. It is clear that even in winter during daylight hours there is sufficient radiation for photolysis to be much faster than the OH reaction. This is also true for the other seasons, so it can be concluded that photolysis is the dominant removal process for nitrosamines and that the OH reaction plays a minor role. It should be noted that both removal processes depend on the amount of solar radiation since the OH radical concentration is directly dependent on photolysis of O_3 and NO_2. When insufficient radiation is available to photolyze the compounds there is also no production of OH radicals (nor production of Cl radicals for example). Precursors of the nitrite radical, NO_3, build up photochemically during the daylight hours and NO_3 oxidizes compounds at night time, but NO_3 production is also dependent on the amount of solar radiation during the day. During dark winter days, when all nitrosamines present are not photolyzed during the day the question is whether there is sufficient of a build-up of NO_3 radicals to oxidize the compounds during the night. In conclusion, nitrosamines are removed rapidly by photolysis when there is sufficient solar UV radiation. During the darkest months the compounds may not be fully removed by photochemistry and it is therefore necessary to carefully consider nitrosamine removal by wet and dry deposition to estimate the lifetime. During the light months of the year nitrosamines are completely removed photochemically in a matter of a few hours.
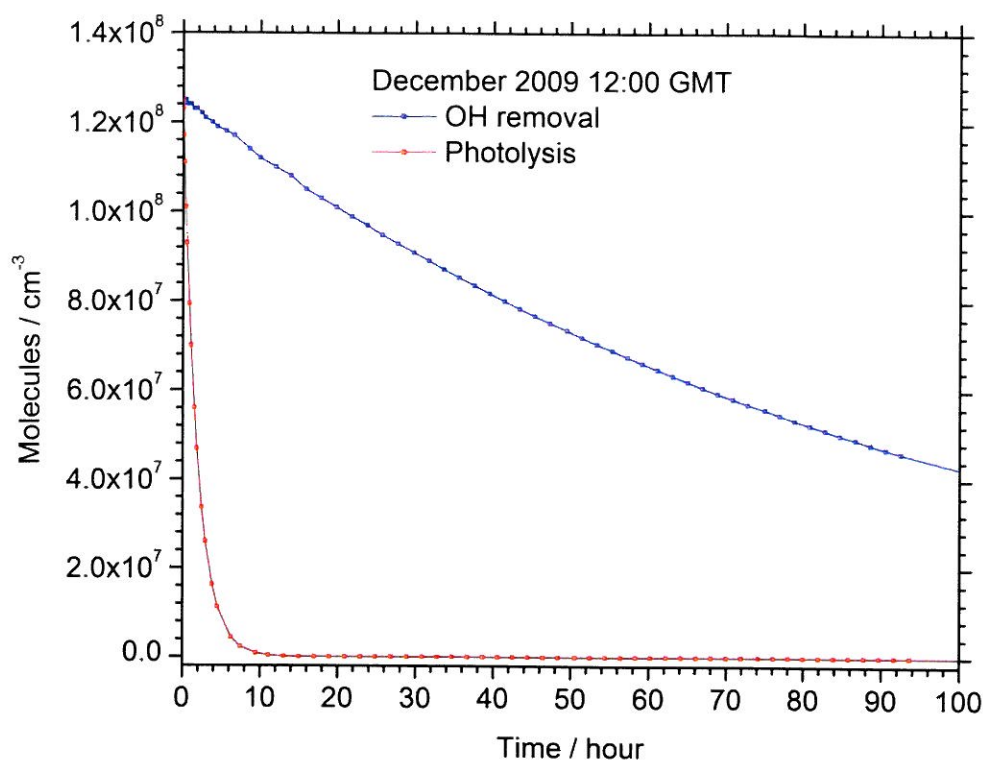
Figure 8: The fate of N-nitrosodimethylamine due to photolysis and reaction with OH at the Mongstad location (0.5 km altitude) midday December 2009 predicted by the one-dimensional tropospheric Kintecus box model.

7 Summary of Assessment

The TD-DFT approach (B3LYP/aug-cc-pVTZ) has shown to provide a reliable method for the prediction of UV-VIS absorption spectral signatures for the class of nitrosamines. Due to the organic $n \rightarrow \pi^*$ chromophore characteristic of nitrosamines, the mean photolysis lifetime for a given solar actinic flux spectrum has the same order of magnitude for all of the target nitrosamines. One exception is 1, 4-dinitrosopiperazine with two degenerate $n \rightarrow \pi^*$ transitions and a shorter mean lifetime. The solar actinic flux spectrum at the environment of the Mongstad location depends highly on the season. The solar actinic flux curves extracted from the Tropospheric Ultraviolet and Visible Radiation Model provided by NCAR show that the photolysis frequencies and mean lifetime with respect to photolysis for the target nitrosamines change by almost an order of magnitude from June to December.

During the summer the mean midday photolysis lifetime is less than 15 min for all target nitrosamines 0.5 km above ground level for the Mongstad location and less than 5 min in the upper troposphere. As such nitrosamine photolysis is the most dominant removal process and other removal channels can be neglected during the daytime. At the equinoxes (March and September) the mean photolysis lifetime has increased to around 30 min at midday but photolysis can still be considered as the major removal process. During the winter the mean lifetime with respect to photolysis at midday has increased to around 2 hours and daily

variation should be considered. At winter solstice (December 22), the photolysis lifetime for the Mongstad location has a minimum of around 2.5 hours around noon and increases rapidly to around 10 hours before the sun sets at 3:30 pm local time and other removal processes need to be considered.

A one-dimensional tropospheric box model including photolysis and OH removal of the nitrosamines has been employed to investigate the importance of these two removal processes at different times of the year. The model results for these different scenarios are considered tentative since accurate values for the rate constants are not available for most of the relevant chemistry. The rate constants have been estimated by employing the one known experimental literature rate constant for the reaction of N-nitrosodimethylamine with OH. The tentative model results show that photolysis is the dominant removal process in all cases but that photochemical removal during the winter is slow and other removal processes should be considered. These include wet and dry deposition and aerosol chemistry.

The present study was not able to identify any previously unknown nitrosamine photolysis degradation products. Photochemical degradation of nitrosamines leads to the formation of peroxyacyl nitrates and amides which have longer lifetimes in the troposphere. The amino radical produced by photolysis can react with O_2 and form amides. Another minor pathway that might be considered is formation of nitramines in the presence of NO_x:

$$R_2N-NO + h\nu \rightarrow R_2N\cdot + NO$$

$$R_2N\cdot + NO_2 \rightarrow R_2N-NO_2$$
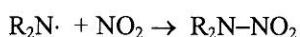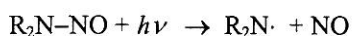
The nitramines formed are not photolyzed in the troposphere and are much longer lived than the nitrosamines. The amino radical may of course also reform the nitrosamine by reaction with NO. The extent to which nitrosamines are converted into longer-lived nitramines depends on the NO_x concentrations. It should be noted however, that high NO_x conditions go hand in hand with high concentrations of radicals in general which will speed up the photochemical removal of all these compounds. An assessment of the frequency of very high NO_x conditions at the Mongstad site will determine whether this is a potential cause for concern.

For the purpose of modelling a generalized expression for determining the photolysis constant is as follows:

$$J = \int I(\nu)\sigma(\nu)\, d\nu$$

where $I(\nu)$ is the solar actinic flux at the desired location and time (units of photons $s^{-1}\, nm^{-1}\, cm^{-2}$) and $\sigma(\nu)$ is the molar extinction coefficient (units of $cm^2\, molecule^{-1}$) of the molecule at a given wavelength. $\sigma(\nu)$ has been determined for a range of wavelengths (= the UV spectrum) for a number of nitrosamines in this study (shown in figure 9.2). The solar flux data can be obtained from the NCAR TUV method or by other methods. For nitrosamines for which $\sigma(\nu)$ is not known we recommend that data for dimethylnitrosamine, the most well-studied of these compounds, can be used as these spectra are all very similar (see figure 9.2).
It is also possible to use the J/J(NO$_2$) factors in table 6 to estimate the J-value in a model, provided J(NO$_2$) can be determined in the model. For dimethylnitrosamine the yearly average J/J(NO$_2$) is 0.14 at Mongstad.

8   References

1. Bamford, C. H., A study of the photolysis of organic nitrogen compounds - Part I Dimethyl- and diethyl-nitrosoamines. *Journal of the Chemical Society* **1939**, 12-17.

2. Tuazon, E. C.; Carter, W. P. L.; Atkinson, R.; Winer, A. M.; Pitts, J. N., Atmospheric reactions of N-nitrosodimethylamine and dimethylnitramine. *Environmental Science & Technology* **1984**, *18* (1), 49-54.

3. Geiger, G.; Huber, J. R., Photolysis of dimethylnitrosamine in the gas phase. *Helvetica Chimica Acta* **1981**, *64* (4), 989-995.

4. Stefan, M. I.; Bolton, J. R., UV direct photolysis of N-nitrosodimethylamine (NDMA): Kinetic and product study. *Helvetica Chimica Acta* **2002**, *85* (5), 1416-1426.

5. NCAR Tropospheric Ultraviolet and Visible (TUV) Radiation Model (http://cprm.acd.ucar.edu/Models/TUV/)..

6. Danielache, S. O.; Eskebjerg, C.; Johnson, M. S.; Ueno, Y.; Yoshida, N., High-precision spectroscopy of ^{32}S, ^{33}S, and ^{34}S sulfur dioxide: Ultraviolet absorption cross sections and isotope effects. *J. Geophys. Res.* **2008**, *113* (D17), D17314.

7. Silva, M. R.; Schreiber, M.; Sauer, S. P. A.; Thiel, W., Benchmarks for electronically excited states: Time-dependent density functional theory and density functional theory based multireference configuration interaction. *J. Chem. Phys.* **2008**, *129* (10).

8. Schreiber, M.; Silva, M. R.; Sauer, S. P. A.; Thiel, W., Benchmarks for electronically excited states: CASPT2, CC2, CCSD, and CC3. *J. Chem. Phys.* **2008**, *128* (13).

9. Frisch, M. J.; Trucks, G. W.; Schlegel, H. B.; Scuseria, G. E.; Robb, M. A.; Cheeseman, J. R.; Scalmani, G.; Barone, V.; Mennucci, B.; Petersson, G. A.; Nakatsuji, H.; Caricato, M.; Li, X.; Hratchian, H. P.; Izmaylov, A. F.; Bloino, J.; Zheng, G.; Sonnenberg, J. L.; Hada, M.; Ehara, M.; Toyota, K.; Fukuda, R.; Hasegawa, J.; Ishida, M.; Nakajima, T.; Honda, Y.; Kitao, O.; Nakai, H.; Vreven, T.; Montgomery, J. A.; Peralta, J. E.; Ogliaro, F.; Bearpark, M.; Heyd, J. J.; Brothers, E.; Kudin, K. N.; Staroverov, V. N.; Kobayashi, R.; Normand, J.; Raghavachari, K.; Rendell, A.; Burant, J. C.; Iyengar, S. S.; Tomasi, J.; Cossi, M.; Rega, N.; Millam, J. M.; Klene, M.; Knox, J. E.; Cross, J. B.; Bakken, V.; Adamo, C.; Jaramillo, J.; Gomperts, R.; Stratmann, R. E.; Yazyev, O.; Austin, A. J.; Cammi, R.; Pomelli, C.; Ochterski, J. W.; Martin, R. L.; Morokuma, K.; Zakrzewski, V. G.; Voth, G. A.; Salvador, P.; Dannenberg, J. J.; Dapprich, S.; Daniels, A. D.; Farkas; Foresman, J. B.; Ortiz, J. V.; Cioslowski, J.; Fox, D. J., Gaussian 09, Revision A.02. Wallingford CT, 2009.

10. Ianni, J. C., A comparison of the Bader-Deuflhard and the Cash-Karp Runge-Kutta integrators for the GRI-MECH 3.0 model based on the chemical kinetics code Kintecus. In *Computational Fluid and Solid Mechanics 2003*, Bathe, K. J., Ed. Elsevier Science Ltd: Oxford, 2003; pp 1368-1372.

11. Ianni, J. C., www.kintecus.com.

12. (a) R. Atkinson, D. B., R. Cox, J. Crowley, R. Hampson, R. Hynes, M. Jenkin, M. Rossi, J. Troe, and T. Wallington, Evaluated Kinetic and Photochemical data for Atmospheric Chemistry:Volume I-IV. *Atmos. Chem. Phys.* **2008**, *8*, 4141-4496; (b) S.P. Sander, R. R. F., D.M. Golden, M.J. Kurylo, G.K. Moortgat, H. Keller-Rudek, P.H. Wine, A.R. Ravishankara, C.E. Kolb, M.J. Molina, B.J. Finlayson-Pitts, R.E. Huie, V.L. Orkin *Chemical Kinetics and Photochemical Data for Use in Atmospheric Studies. Evaluation Number 15, JPL Publication 06-2*; Jet Propulsion Laboratory, Pasadena: 2006.

13. Seinfeld, J. H.; Pandis, S. N., *Atmospheric chemistry and physics: from air pollution to climate change*. John Wiley & Sons, Inc.: Hoboken, 2006; p xxviii + 1203.
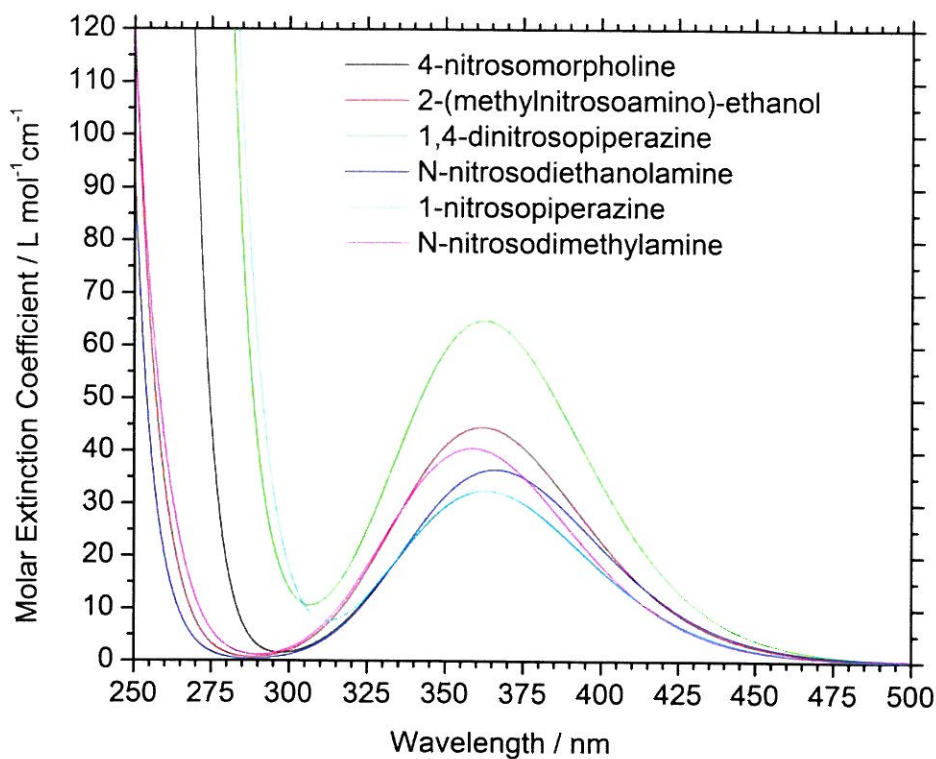
9 Appendices

9.1 Appendix A: The daily variation of the actinic solar flux at the Mongstad plant during winter solstice conditions (December 22, 2009).
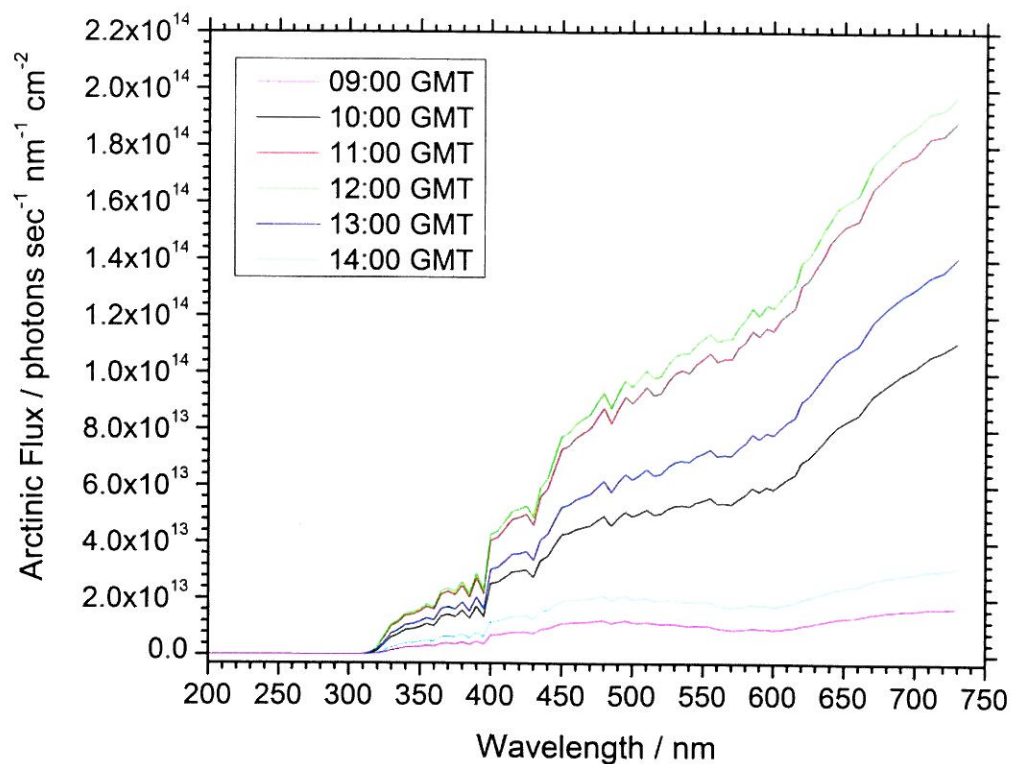
9.2 Appendix B: Simulation of UV-VIS absorption spectra for the target nitrosamines predicted by the B3LYP/aug-cc-pVTZ level of theory (TD-DFT approach).

SINTEF

9.3 Appendix C: The overlap region of the solar actinic flux curve (June 2010) and the simulated UV-VIS absorption spectrum (B3LYP/aug-cc-pVTZ) of N-nitrosodimethyl-amine.
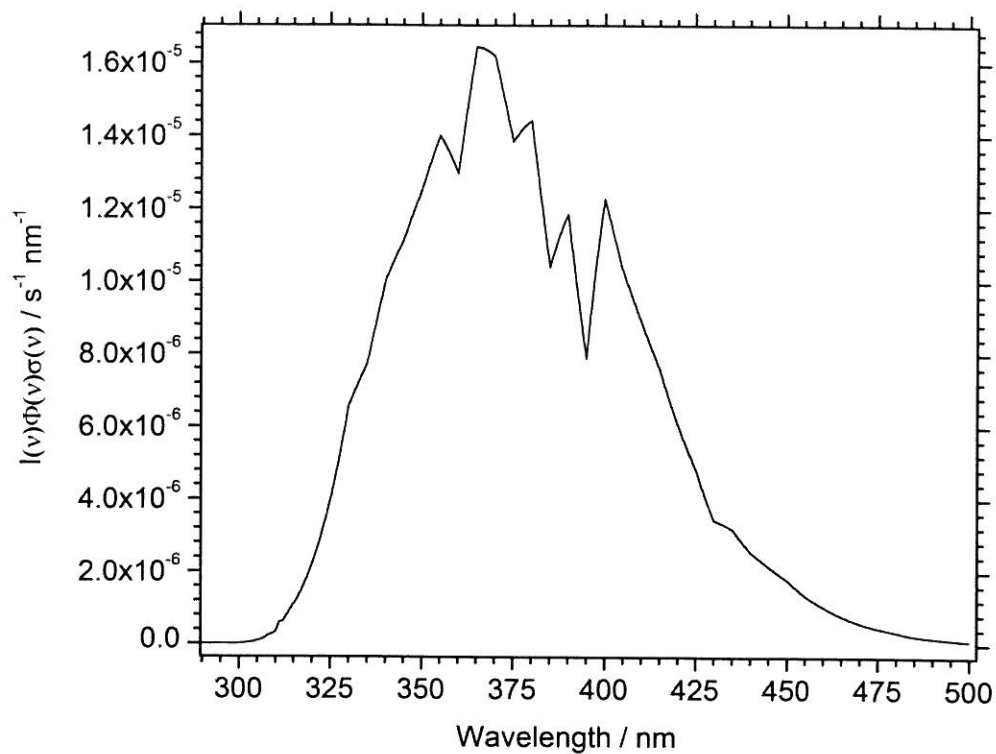
9.4 Appendix D: The daily variation of the photolysis frequency and mean photolysis lifetime for N-nitrosodimethylamine at the Mongstad location during winter solstice (Dec. 22, 2009).

Time / Altitude / km	Photolysis Frequency J / s^{-1}	Mean Photolysis Lifetime τ / hour
09:00 GMT / 0.5	1.9×10^{-5}	14.9
10:00 GMT / 0.5	6.8×10^{-5}	4.1
11:00 GMT / 0.5	1.1×10^{-4}	2.6
12:00 GMT / 0.5	1.2×10^{-4}	2.4
13:00 GMT / 0.5	8.1×10^{-5}	3.4
14:00 GMT / 0.5	3.1×10^{-5}	8.9

SINTEF

Technology for a better society
www.sintef.no